Optimal Control for Resource Allocation in a Multi-Patch Epidemic Model with Human Dispersal Behavior

A.U.S. Adikari[1*], **Y. Jayathunga**[1]

[1]Department of Mathematics, Faculty of Science, University of Colombo, Colombo 03, Sri Lanka

[*]Email: udaniiadikari@gmail.com

Abstract

A multi-patch epidemic compartmental model with human dispersal behavior studies the spread of the disease and it sets the model to real-world situations. The mobility matrix (M) applies human dispersal behavior to the model. The optimal control theory assists in controlling the disease burden while minimizing the cost of infected individuals and implementing control measures. We formulate a multi-patch SIR model with human dispersal behavior to control and reduce communicable disease outbreaks such as COVID-19 by optimizing resource allocation in Sri Lanka. Results are represented by using the reproduction number (R_0), effective reproduction number (R_t), and final epidemic size (c_i). Compared to the basic reproduction number (R_0), the effective reproduction number (R_t) represents the significant result in the epidemiological model incorporated with control measures. The average number of secondary cases concerning the current susceptible population is represented by R_t and the final epidemic size represents the patched-specified cost value for infected individuals. According to the results, the disease burden can be controlled by vaccination relative to social distancing.

Keywords: Multi-patch model, human dispersal, optimal control, effective reproduction number, vaccination, social distancing

2020 MSC classification number: 37N35, 37N30, 49J15, 92D30, 93C15, 93A30

1. INTRODUCTION

Compartmental models are widely used to model the transmission of diseases [1]. Traditional models consider only a closed population within a patch. However, in a real-world scenario, it is significant to study the spread of the disease in multi-patch [2]. Human dispersal behaviors significantly influence the transmission of diseases because it is facilitated to interconnect the geographical or sociological distinct areas [3]. The optimal control theory is employed to identify the appropriate control strategies to reduce the size of the outbreak and decrease the number of infected individuals while minimizing the costs of implementing the control strategies [4]. The mathematical modeling and analysis of epidemic models with optimal control theory can be found in communicable diseases such as Rabies, Dengue, Malaria, Zika, Ebola, and COVID-19 [5], [6], [7], [8], [9], [12]. Drug distribution, quarantine, vaccination, self-protection policies (such as hand hygiene, face masks, sanitizers), and social distancing are examples of resources [1], [7], [13], [14].

The SARSCoV-2 virus caused the Coronavirus disease 2019 (COVID-19) [15]. It originated in December 2019 in Wuhan City, Hubei Province, China, and spread over 229 countries [15]. It is primarily transmitted when virus-containing droplets, aerosols, and airborne particles in the air and facilitates human-to-human transmission [15]. The disease globally spreads through human mobility. The World Health Organization (WHO) declared a pandemic in March 2020 [15]. In the initial stages of the novel disease, there are no specific or identified control or prevention strategies. According to WHO guidelines, countries have implemented several control strategies such as self-protection policies (hand hygiene, face masks, sanitizers, etc.), social distancing, self-quarantine, mandatory quarantine (private residences, hospitals, public institutions, etc.), and restrictions on human movements [16]. As of September 01, 2023, COVID-19 has resulted in 770,085,713 confirmed cases and 6,956,173 deaths worldwide [17].

The first confirmed case involving a Chinese tourist in Sri Lanka was reported on January 27, 2020, followed by the first local case on March 11, 2020 [18]. To control the situation, the government implemented a strict

*Corresponding author

Received May 1^{st}, 2024, Revised November 29^{th}, 2024, Accepted for publication December 20^{th}, 2024. Copyright ©2025 Published by Indonesian Biomathematical Society, e-ISSN: 2549-2896, DOI:10.5614/cbms.2025.8.1.1

nationwide lockdown on March 20, 2020, to reduce the contact rate [19]. During this period, people faced several financial challenges due to economic failures locally and globally. On April 19, 2020, the government announced the relaxation of the strict lockdown by considering the spread of the disease as well as economic failure [19]. Inter-district travel was permitted only for essential service purposes. As of May 11, 2020, the country had partially reopened to offices and businesses under a set of health regulations such as self-protection policies and social distancing [19]. But after much more time the government had to announce the strict nationwide lockdown and partial lockdown due to the spread of the disease [19]. Worldwide distribution of COVID-19 vaccinations began on December 08, 2020 [20]. Commencing on January 29, 2021, vaccination programs were initiated in Sri Lanka [21].

The initial epidemic model was proposed by Kermack and McKendrick in 1927, known as the SIR epidemic model [4]. The model was developed under the following assumptions: infected individuals are also infectious, the population is closed, no one from the outside enters the population and no one leaves the population and there are no births and deaths in the population and all recovered individuals have complete immunity and cannot be infected again.

To model the behavior of the transmission of diseases in multi-patch and multi-group or age-structure, Ross introduced a contact matrix in 1911 [22]. This matrix is used to collect re-scaled estimated levels of activity among interacting subgroups or age classes in heterogeneous mixing populations and captures the spatial spread of disease by using the Eulerian framework [23]. In 1955, S. Rushton and A. J. Mautner defined a deterministic model for more than one community, which was a more realistic model [24].

A patch residence-time matrix P is defined as the function of the human virtual dispersal behavior in the Lagrangian framework [25]. The risk of infection is a function of the residence time and local environmental risk. The transmission rate (β) per unit of time is used to rank patch-dependent risks of infection. The Lagrangian approach is introduced here to avoid assigning heterogeneous contact rates. Defining and measuring the contact rate in communicable diseases is more difficult due to the factors that incorporate the spreading of the disease. An infection risk vector indicates an environmental risk to a pre-specified disease (measured by B) for a particular patch. Together the infected risk vector (B) and residence time matrix (P) play a major role in the spreading of the diseases.

In one patch model, they address one or more control strategies to reduce the disease burden. To minimize the disease burden of Ebola and the effectiveness of vaccination on infected populations they used control strategies such as hospitalization, quarantine, and vaccination [8]. A paper on Zika, a sexually transmitted disease, and control strategies such as personal protection, condom use, vaccination, treatment, and spraying of insecticide had been published to minimize the disease burden and cost of control measures [6]. A model is developed for COVID-19 based on the SIVR-type incorporated with control variables such as vaccination strategy, quarantine, reduction of vaccine shrinkage, and treatment [26]. According to the following paper, after introducing control strategies, the spread of the disease in India and the USA was reduced by 50% and 100% respectively [27]. Here they used control strategies such as quarantining (susceptible, exposed, and infected) populations and vaccinating the entire population.

To formulate an accurate model, it is important to derive a model considering the multi-patch [1], [2], [5], [23], [24], [25], [28], [29]. Previous works on a two-patch model incorporated with optimal strategies were studied on Dengue transmission dynamics and COVID-19 [1], [29]. To determine the optimal timing for distributing vaccines in the meta-population of Raccoons against Rabies, optimal control theory was applied [5]. Another model for Dengue transmission in multi-patch was constructed by incorporating optimal control theory and mobility via the residence-time budgeting matrix [30]. An age-structured model was formulated to allocate the vaccination by considering the age distribution of Sri Lanka optimally [31]. A study was done based on different mobility patterns and geographically provincial patches.

For this research, the selected population is Sri Lanka and the patches are based on geographical provinces: Northern, North Western, Western, North Central, Central, Sabaragamuwa, Eastern, Uva, and Southern [32]. The mobility matrix is used for interconnecting these patches. The control measures were defined according to the guidelines from the WHO. In this research, we aimed to propose a multi-patch SIR model with human dispersal behavior and used optimal control theory for identifying control strategies and allocating resources optimally.

The organization of this paper can be summarized as follows: The steps of the proposed model formulation, reproduction number, effective reproduction number, and final epidemic size for the model are derived in Section 2. Computational results of the model are discussed in Section 3. Section 4 presents the discussion of the results.

2. MODEL FORMULATION

The ordinary differential equations (ODE) system that introduces human mobility to the epidemic model can be found in the following previous works [2], [25], [28]. This model was developed under the following assumptions: There is homogeneous mixing within each community with α_i as the internal infection rate in the i^{th} community and there is also homogeneous mixing between communities with β_j as the infection rate between the i^{th} and j^{th} communities. The multi-patch SIR model follows the ODE system [2], [25],

$$\begin{aligned} S_i' &= -S_i \sum_{j=1}^{n} \beta_j P_{ij} \frac{\sum_{k=1}^{n} P_{kj} I_k}{\sum_{k=1}^{n} P_{kj} N_k}, & S(t_0) = S_0 \geq 0, \\ I_i' &= S_i \sum_{j=1}^{n} \beta_j P_{ij} \frac{\sum_{k=1}^{n} P_{kj} I_k}{\sum_{k=1}^{n} P_{kj} N_k} - \alpha_i I_i, & I(t_0) = I_0 \geq 0, \\ R_i' &= \alpha_i I_i, & R(t_0) = R_0 \geq 0, \end{aligned} \tag{1}$$

where $\sum_{j=1}^{n} P_{ij} = 1$, $i = 1, 2, ..., n$ and n is the number of patches.

Here S_i, I_i, and R_i represent the number of susceptible, infected, and recovered individuals in patch i respectively at time t with constant population. The β_i is the environmental risk of patch i (Transmission rate), α_i is the recovery rate, P_{ij} is the probability of moving an infected individual from patch i to j and N_i is the population of i^{th} patch.

2.1. Proposed model

The boundary lines of the proposed model are described in Section 1. The proposed model is defined based on the multi-patch SIR model described in Equation 1. The key assumptions are used to formulate the model: the birth and death rates are negligible due to the short period, and the total population remains the same. The N_i is the same as the initial total population of each patch and is Unchanged. All recovered individuals have complete immunity and cannot be infected again. The recovery rate (α_i) for all patches is considered as α due to Sri Lanka being a small country [10]. Assume that $0 \leq u_{1i}, u_{2i} \leq 0.8$, because the total controlling is not possible [11]. The ODE system for the proposed model is as follows,

$$\begin{aligned} S_i' &= -S_i \sum_{j=1}^{n} \beta_j (1 - u_{1i}) P_{ij} \frac{\sum_{k=1}^{n} P_{kj} I_k}{\sum_{k=1}^{n} P_{kj} N_k} - u_{2i} S_i, & S(t_0) = S_0 \geq 0, \\ I_i' &= S_i \sum_{j=1}^{n} \beta_j (1 - u_{1i}) P_{ij} \frac{\sum_{k=1}^{n} P_{kj} I_k}{\sum_{k=1}^{n} P_{kj} N_k} - \alpha_i I_i, & I(t_0) = I_0 \geq 0, \\ R_i' &= \alpha_i I_i + u_{2i} S_i, & R(t_0) = R_0 \geq 0, \end{aligned} \tag{2}$$

where $0 \leq u_{1i}, u_{2i} \leq 0.8, \quad \sum_{i=1}^{n} P_{ij} = 1 \quad and \quad i = 1, 2, ..., n.$

Here P_{ij} is the proportion of susceptible individuals from Patch i who are currently in Patch j, u_{1i} is the cost of social distancing, quarantine, PCR tests, and related medical costs per unit of time for patch i. For ease of notation, we have renamed u_{1i} control strategies as the cost of social distancing per unit of time for patch i. The u_{2i} is the cost of vaccination per unit of time for patch i. Definitions of the parameter are shown in Table 1. Figure 1 illustrates the proposed multi-patch compartmental model with control strategies.

The term of $(1 - u_{1i})$ is directly affected by the transmission rate. By setting u_{1i} to 1, the maximum social distancing measure is achieved. A real-world example would be a situation where social distancing is strictly applied, corresponding to a full lockdown situation. Under these conditions, the term $(1 - u_{1i})$ becomes zero, effectively affecting the transmission rate associated with it $\left(\sum_{j=1}^{n} \beta_j (1 - u_{1i}) P_{ij} \frac{\sum_{k=1}^{n} P_{kj} I_k}{\sum_{k=1}^{n} P_{kj} N_k}\right)$. When $u_{1i} = 0$, it indicates that there are no mobility restrictions, allowing daily human dispersal behaviors.

Table 1: Parameter definition of the proposed model.

Symbol	Parameter definition
S_i	The number of susceptible individuals in patch i
I_i	The number of infected individuals in patch i
R_i	The number of recovered individuals in patch i
n	The number of patches
β_i	The environmental risk of patch i (Transmission rate)
P_{ij}	The probability of moving infected individual from patch i to j
α_i	The recovery rate of patch i
N_i	The total population of i^{th} patch
u_{1i}	The cost of social distancing, quarantine, Polymerase Chain Reaction (PCR) tests, and related medical costs per unit of time for patch i
u_{2i}	The cost of vaccinated per unit of time in patch i

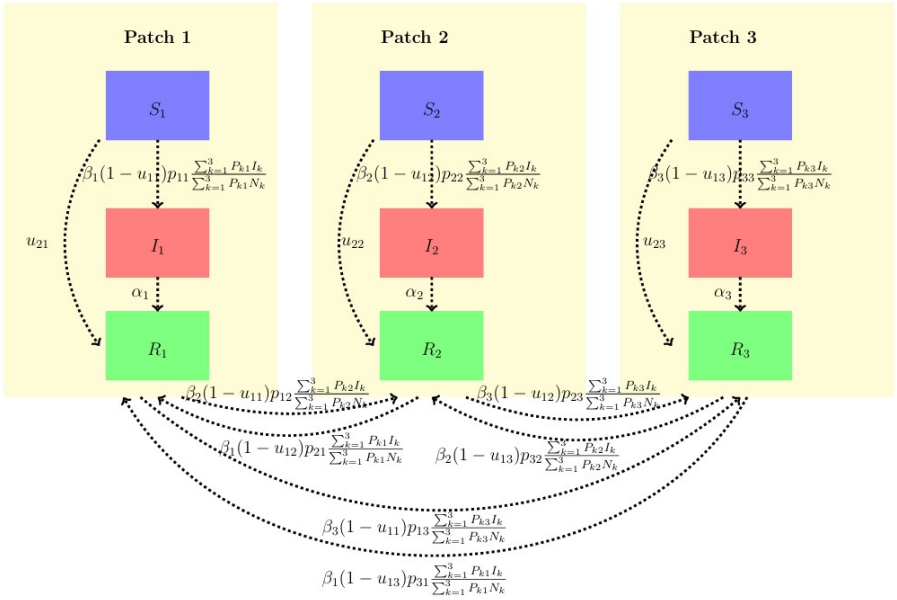

Figure 1: The proposed compartment model for 3 patches mathematically described in Equation 2.

Vaccination helps to improve the immunity of the human body. Moreover, the control measures u_{2i} control the rate of susceptible individuals becoming infectious in patch i. When increasing the value of u_{2i}, increase the number of vaccinated susceptible individuals and they move into the recovery class. The goal is to minimize the number of infected individuals in each patch at a minimal cost of implementation over a finite time.

Objective Functional,

$$\min_{U} J(U) = \min_{u_{1i},u_{2i}} \int_0^T \sum_{i=1}^{n} \left(a_i I_i + \frac{b_i}{2} {u_{1i}}^2 + \frac{c_i}{2} {u_{2i}}^2 \right) dt. \tag{3}$$

Equation 3 represents the objective functional, while Equation 2 represents the subject of the states. Here a_i is the positive constant of the costs per treatment of the infected individual in patch i. The b_i and c_i are relative cost of the implementation of controls for patch i, u_{1i} and u_{2i} respectively. Pontryagin's Maximum Principle is the fundamental theory for solving the optimal control problem [12]. The necessary condition is defined according to Pontryagin's Maximum Principle.

Hamiltonian H is defined as, $H = \sum_{i=1}^{n} \left(a_i I_i + \frac{b_i}{2} {u_{1i}}^2 + \frac{c_i}{2} {u_{2i}}^2 + \lambda_{1i} S_i' + \lambda_{2i} I_i' + \lambda_{3i} R_i' \right)$. There exist adjoint variables λ_{1i}, λ_{2i}, λ_{3i} where $i = 0, ...n$ which satisfy the system of ODE in Sub-section 2.1,

$$\begin{aligned}
\lambda_{1i}' &= -\frac{dH}{dS_i} \\
&= (\lambda_{1i} - \lambda_{2i}) \left(\sum_{j=1}^{n} \beta_j (1 - u_{1i}) P_{ij} \frac{\sum_{k=1}^{n} P_{kj} I_k}{\sum_{k=1}^{n} P_{kj} N_k} \right) + (\lambda_{1i} - \lambda_{3i}) u_{2i}, \\
\lambda_{2i}' &= -\frac{dH}{dI_i} \\
&= -a_i + (\lambda_{1i} - \lambda_{2i}) S_i \left(\sum_{j=1}^{n} \beta_j (1 - u_{1i}) P_{ij} \frac{P_{ij}}{\sum_{k=1}^{n} P_{kj} N_k} \right) + \alpha (\lambda_{2i} - \lambda_{3i}), \\
\lambda_{3i}' &= -\frac{dH}{dR_i} = 0,
\end{aligned}$$

with the transversality conditions, $\lambda_{1i}(t) = \lambda_{2i}(t) = \lambda_{3i}(t) = 0$. The optimality controls u_{1i}, u_{2i} are derived by the optimality condition 4,

$$\begin{aligned}
\frac{dH}{du_{1i}} &= 0, \\
\frac{dH}{du_{2i}} &= 0.
\end{aligned} \tag{4}$$

The optimality control variables (u_{1i}^*, u_{2i}^*) are given by,

$$\begin{aligned}
u_{1i}^* &= \min \left\{ 0.8, \max \left\{ 0, \frac{(\lambda_{2i} - \lambda_{1i}) \left(\sum_{j=1}^{n} \beta_j \frac{\sum_{k=1}^{n} P_{kj} I_k}{\sum_{k=1}^{n} P_{kj} N_k} \right)}{b_i} \right\} \right\}, \\
u_{2i}^* &= \min \left\{ 0.8, \max \left\{ 0, \frac{(\lambda_{2i} - \lambda_{3i}) S_i}{c_i} \right\} \right\}.
\end{aligned}$$

2.2. Basic reproduction number, effective reproduction number, and the final epidemic size

The basic reproductive ratio or basic reproduction number, R_0 represents the significant result in the epidemiological model. R_0 is the average number of infectious secondary cases when one infectious individual has originated in the susceptible population [1]. By using the Next Generation Method, R_0 is computed [4]. An epidemic occurs when $R_0 > 1$, and an endemic occurs when $R_0 = 1$ [4].

The next generation matrix K is defined by,

$$K = -FV^{-1}, \quad \text{where} \quad F = \left[\frac{\partial f_i(x_0)}{\partial x_j} \right] \quad \text{and} \quad V = \left[\frac{\partial v_i(x_0)}{\partial x_j} \right], \tag{5}$$

$f_i(x)$ be the rate of appearance of new infections in compartment i, $v_i(x)$ is the difference between the rate of transfer of individuals into and out of compartment i. The difference of $f_i(x) - v_i(x)$ gives the rate of change of x_i. Here x_i denotes the number or proportion of individuals in the i compartment, x_0 is the disease-free equilibrium point (DFE point) and $i, j = 1, ..., m$ [4], [33]. At the point of DFE, there are no infected individuals. Then R_0 is given by,

$$Ro = \max \{ \text{eigenvalue}(K) \}. \tag{6}$$

We formulate the basic reproduction number according to the model described in Equation 2. $f_i(I)$ and $v_i(I)$ are defined for our model according to the Equation 5,

$$f_i(I) = \begin{pmatrix} S_1(t)\sum_{j=1}^{n} B_j(1-u_{11})P_{ij}\dfrac{\sum_{k=1}^{n} P_{kj}I_k(t)}{\sum_{k=1}^{n} P_{kj}N_k(t)} \\ S_2(t)\sum_{j=1}^{n} B_j(1-u_{12})P_{ij}\dfrac{\sum_{k=1}^{n} P_{kj}I_k(t)}{\sum_{k=1}^{n} P_{kj}N_k(t)} \\ \vdots \\ \vdots \\ S_n(t)\sum_{j=1}^{n} B_j(1-u_{1n})P_{ij}\dfrac{\sum_{k=1}^{n} P_{kj}I_k(t)}{\sum_{k=1}^{n} P_{kj}N_k(t)} \end{pmatrix}, \quad -v_i(I) = \begin{pmatrix} \alpha I_1 \\ \alpha I_2 \\ \vdots \\ \vdots \\ \alpha I_n \end{pmatrix}.$$

F and V are defined at the point of DFE, $E_1 = (S_1, I_1, R_1, \ldots, S_n, I_n, R_n) = (N_1, 0, 0, \ldots, N_n, 0, 0)$ according to the mention in Equation 5,

$$F = \begin{pmatrix} \sum_{j=1}^{n} B_j(1-u_{11})P_{1j}\frac{P_{1j}}{\sum_{k=1}^{n} P_{kj}N_k(t)} & \cdots \sum_{j=1}^{n} B_j(1-u_{19})P_{1j}\frac{P_{9j}}{\sum_{k=1}^{n} P_{kj}N_k(t)} \\ \vdots & \vdots \\ \sum_{j=1}^{n} B_j(1-u_{19})P_{9j}\frac{P_{9j}}{\sum_{k=1}^{n} P_{kj}N_k(t)} & \cdots \sum_{j=1}^{n} B_j(1-u_{99})P_{9j}\frac{P_{9j}}{\sum_{k=1}^{n} P_{kj}N_k(t)} \end{pmatrix},$$

$$\text{-}V = \begin{pmatrix} \alpha & \ldots & 0 \\ \vdots & \ddots & \vdots \\ 0 & \ldots & \alpha \end{pmatrix}, \quad -V^{-1} = \frac{1}{\alpha}\begin{pmatrix} 1 & \ldots & 0 \\ \vdots & \ddots & \vdots \\ 0 & \ldots & 1 \end{pmatrix}.$$

Then the next generation matrix $K \in \mathbb{R}^{9\times 9}$,

$$\begin{aligned} K &= -FV^{-1} \\ &= \frac{1}{\alpha}\begin{pmatrix} \sum_{j=1}^{n} B_j(1-u_{11})P_{1j}\frac{P_{1j}}{\sum_{k=1}^{n} P_{kj}N_k(t)} & \cdots \sum_{j=1}^{n} B_j(1-u_{19})P_{1j}\frac{P_{9j}}{\sum_{k=1}^{n} P_{kj}N_k(t)} \\ \vdots & \vdots \\ \sum_{j=1}^{n} B_j(1-u_{19})P_{9j}\frac{P_{9j}}{\sum_{k=1}^{n} P_{kj}N_k(t)} & \cdots \sum_{j=1}^{n} B_j(1-u_{19})P_{9j}\frac{P_{9j}}{\sum_{k=1}^{n} P_{kj}N_k(t)} \end{pmatrix}. \end{aligned}$$

R_0 is given by the largest eigenvalue of K mentioned in Equation 6.

During the epidemic, a proportion of susceptible individuals become infected or immune. The effective reproduction number (R_t) is an approach to capture the actual average number of secondary cases per primary case (current susceptible population) [34]. When estimating R_t, it captures the impact of control measures and non-susceptible individuals in the population [35]. So the value of R_t is lower than the value of R_0.

$$R_t = R_0 x, \tag{7}$$

where R_0 is the basic reproduction number and x is the fraction of the host population (that is susceptible) [36]. The effective reproduction number indicates a more sensitive value than the basic reproduction number when the outbreak is controlled by using a control measure [35]. To analyze the results, we used R_t mentioned in Equation 7.

Under the assumption that all susceptible individuals do not become infectious during an epidemic, we estimate the size of the total infected population [1]. When control measures are incorporated into the epidemic model, the final epidemic size can be used as an indicator. Furthermore, it indicates the impact of control measures [1]. The cumulative number of newly infected cases (or the final epidemic size) numerically by solving the following equation according to the model defined in Equation 1,

$$C_i' = S_i \sum_{j=1}^{n} \beta_j P_{ij} \frac{\sum_{k=1}^{n} P_{kj}I_k}{\sum_{k=1}^{n} P_{kj}N_k}.$$

Patch-specific final epidemic size $(C_i(t_f))$ is indicated as the cumulative number of newly infected cases in patch i. We derived the final epidemic size 8 for the model described in Equation 2 is followed as,

$$C_i' = S_i \sum_{j=1}^{n} \beta_j (1 - u_{1i}) P_{ij} \frac{\sum_{k=1}^{n} P_{kj} I_k}{\sum_{k=1}^{n} P_{kj} N_k}. \tag{8}$$

3. Experimental Results

Reported COVID-19 cases and vaccination data were collected from the Epidemiological Unit in Sri Lanka [37]. Data collected from the Ministry of Finance Sri Lanka was used to estimate the parameters associated with the costs of control measures [38]. The National Transport Commission of Sri Lanka provided mobility data. Province-wise population is on the report of Economic and Social Statistics - 2020, the Central Bank of Sri Lanka.

3.1. Fixed parameter values and estimated parameter Values

Definitions of parameters of the proposed model are shown in Table 1. According to the definitions, values are defined in Table 2.

Table 2: Parameter values.

Symbol	Reference
β_i	Estimated
P_{ij}	Estimated
α	$1/10.25 days^{-1}$ [7]
n	9 [32]

In this case, n equals 9 because Sri Lanka is made up of 9 provinces. By using the number of infected individuals we estimate the transmission rate (β_i) for each province. The nonlinear least squares (NLS) function is used to minimize the sum of the squares of the differences between the actual values and the predicted values. Python contains the **optimize** package in its library **SciPy**. To compute the NLS function by using the inbuilt function '`least_squares()`'. Parameters inside the inbuild function, 'bound' and 'method' should be specified to achieve an accurate transmission rate. The 'trf' is used as a method parameter inside the '`least_squares()`'. The 'trf' is used for problems with bounds [39]. Lower bounds are defined as 0.0001 and upper bounds are defined as infinity. Estimated parameter values for transmission rate (β_i) are shown in Table 3.

Table 3: Estimated values of transmission rate (β_i) described in Section 2.

Symbol	Province	Value
β_1	Northern province	0.09226
β_2	North Western province	0.00867
β_3	Western province	0.16322
β_4	North Central province	0.00970
β_5	Central province	0.00072
β_6	Sabaragamuwa province	0.00065
β_7	Eastern province	0.00442
β_8	Uva province	0.00010
β_9	Southern province	0.00026

In Sri Lanka, the Western province is the most commercially active and busiest province. Every day, more than a thousand of people travel into and out of the province for a variety of reasons, including work, education, and commercial activity. Moreover, it has the highest population density. The transmission rate of the Western province is estimated at high values because of the above-mentioned reasons.

The P_{ij} is constructed by available bus data in the National Transport Commission of Sri Lanka under the following assumptions due to the lack of mobility data [40], [41]. Initially, we have a number of passengers who use buses as their transportation modes province-wise. To calculate the mobility matrix, we assume that other modes of transport such as trains will contribute at proportions corresponding to their use.

3.2. Results in the absence of control measures

Before analyzing the model described in Equations 2 and 3, we analyze the spreading of the disease in the long run. As shown in Figure 4, the disease takes nearly 1000 - 1250 days (nearly 3 to 4 years) to control without any control measures. According to the following Figure 2, $R_0 = 1.1$ which indicates a pandemic situation. A detailed representation of disease spread by using R_t with time is shown in Figure 3. After nearly 750 to 1000 days without any control strategies, R_t gradually decreases to 1.0. At that point, the disease has been controlled but does not die out.

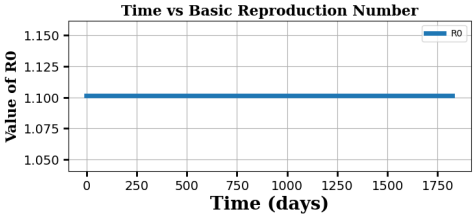

Figure 2: Basic reproduction number over time without any control measures.

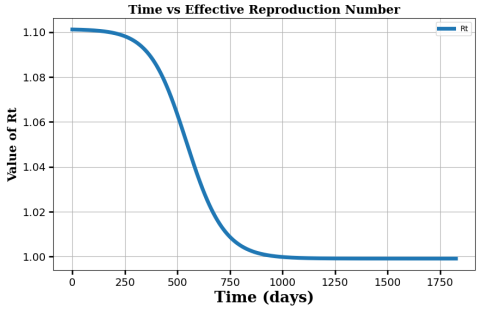

Figure 3: Effective reproduction number over time without any control measures.

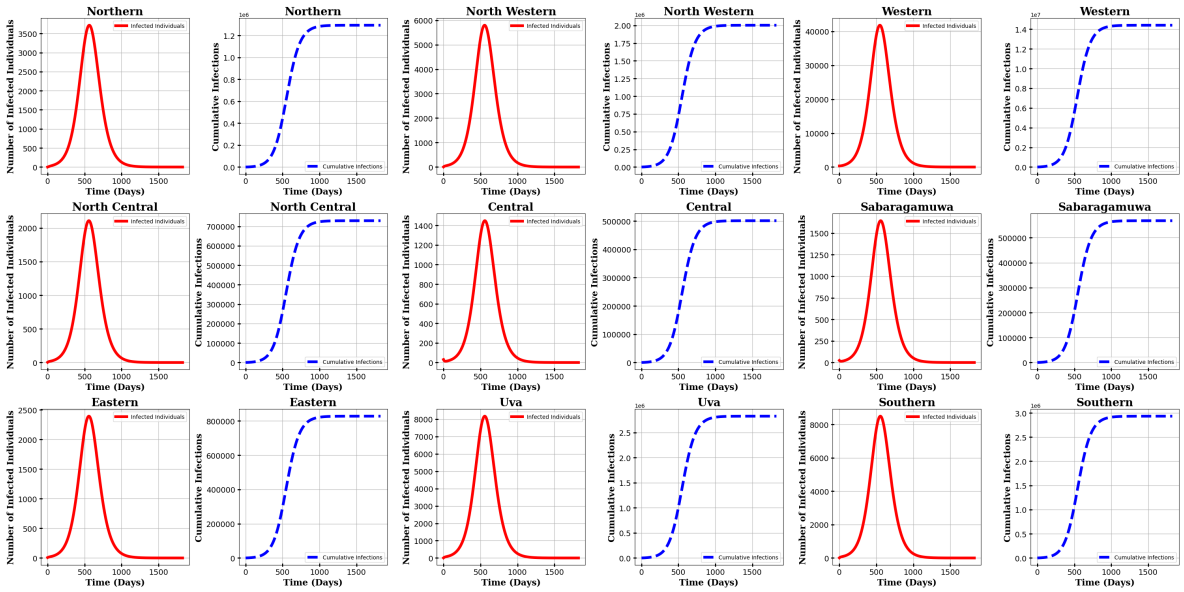

Figure 4: **Red lined** plot- infected individuals over time and **Blue dashed-lined** plot- Cumulative sum of infected individuals (Final epidemic size) over time, without any control measures respective to provinces.

For the first 450 to 700 days the spreading rate increases and when it reaches the peak value, then the spreading rate decreases. In Figure 4, red-lined plots show the infected individuals over time, and blue dashed-lined plots show the cumulative sum of infected individuals (final epidemic size) over time without any control measures respective to provinces, Northern, North Western, Western, North Central, Central, Sabaragamuwa, Eastern, Uva, and Southern. Almost 1000 days are required to control the disease, which is a long period. Disease spread negatively impacts the public health system as well as the economy of the

country. The disease must be controlled within a minimum disease burden, so that the spread of the disease may be controlled.

3.3. Results in the presence of control measures separately

The need for control measures is described in sub-section 3.2. This section analyzes the behavior of disease spreading considering the control measures separately.

1) ***Only considering the social distancing as a control measure****:* The goal is to reduce the disease burden while minimizing the cost associated with the control measure (social distancing) and infectious individuals. Since COVID-19 is a novel disease, in the initial stage there are no disease-specified control measures. Taking into account the WHO guidelines, the government implements social distancing in order to reduce the disease burden.

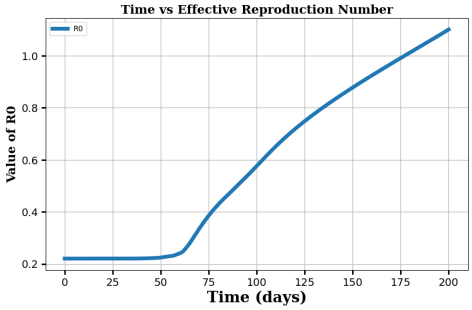

Figure 5: Effective reproduction number when social distancing is used as a control measure.

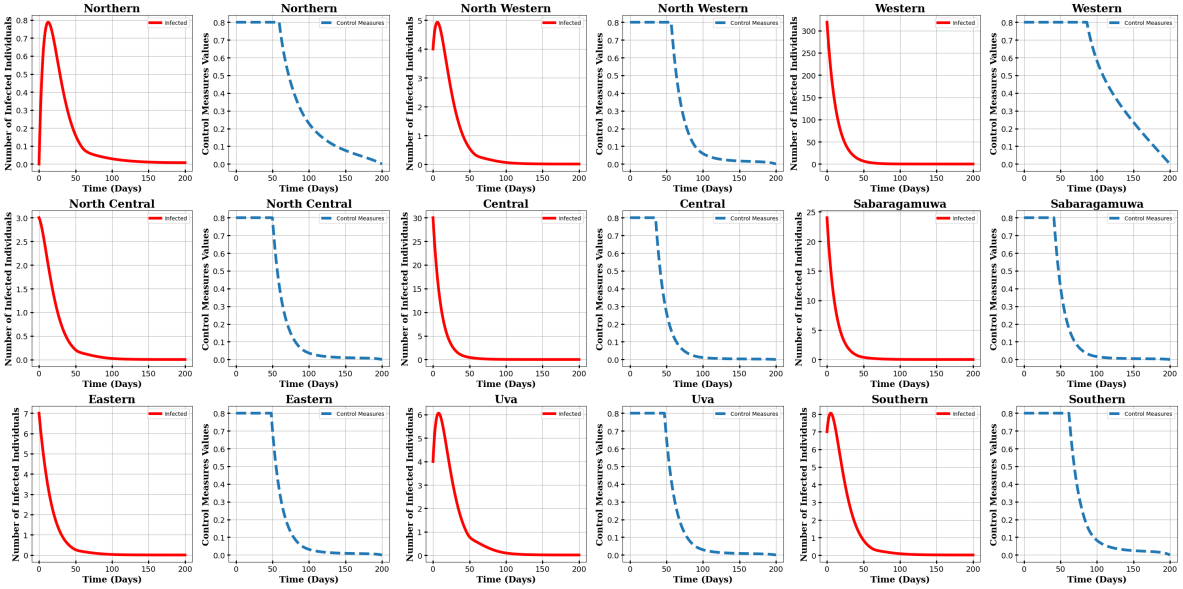

Figure 6: **Red lined** plot - infected individuals over time and **Blue dashed-lined** plot - the value of u_{1i} control measures over time respective to provinces.

According to Figure 6, red-lined plots show the number of infected individuals over time, and blue dashed-lined plots are the corresponding values of control measure (u_{1i}). Reduce the number of infected individuals

with optimal control, takes a minimum of 150 days. By implementing the maximum control measure it takes 50-80 days to control the disease burden. Due to various economic crises, 50 days of full lockdown and 50 - 80 partial lockdown are not appropriate in a low-income country such as Sri Lanka. As u_{1i} appears to have its maximum capacity during the initial days, R_t indicates the lower value. The value of u_{1i} gradually decreases when R_t value gradually increases, as can be observed in Figure 5. Additionally, social distancing can only control the disease burden, and it fails to reach an endemic.

2) ***Only considering the vaccination as a control measure****:* In the initial stage, the system indicates a pandemic situation. Figure 7 shows the effective reproduction number (R_t) varies with time and gradually decreases to zero. Due to the fact that vaccines contribute to the improvement of immunity within the human body, vaccinations control suspect individuals being infected individuals. The R_t represents the sensitive representation of the prediction of the secondary cases as described in the sub-section 2.2.

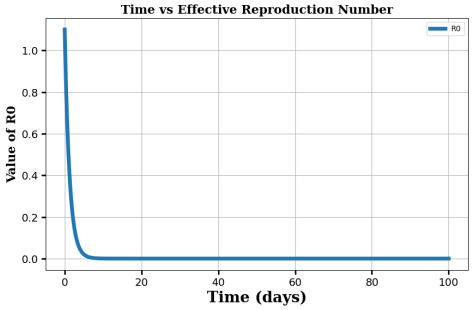

Figure 7: Effective reproduction number when vaccination is used control measure

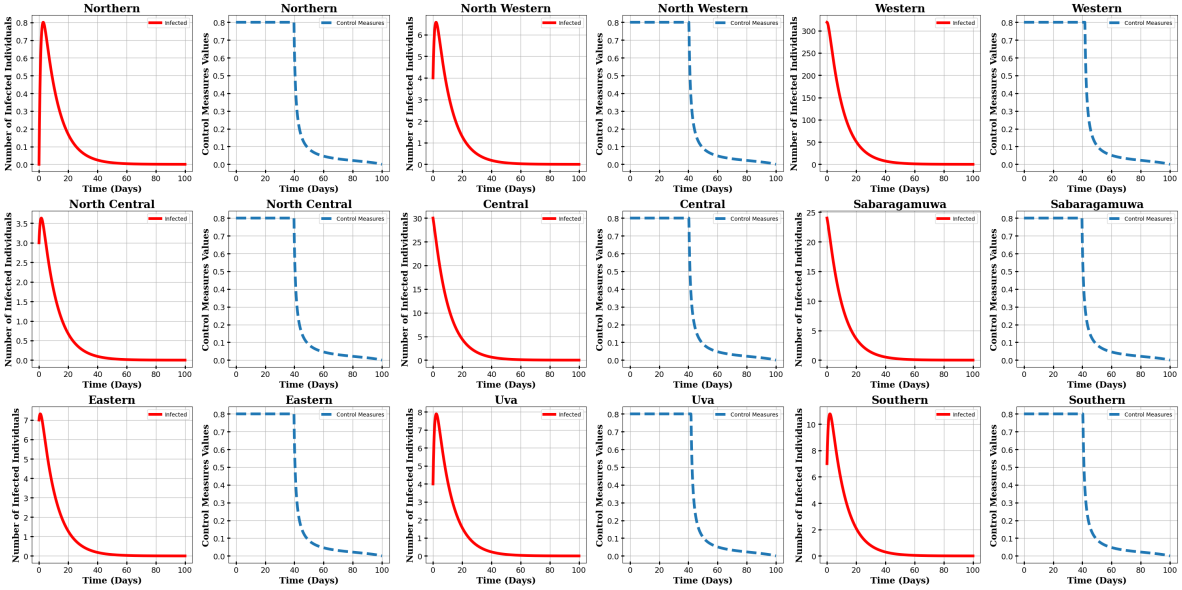

Figure 8: **Red lined** plots - infected individual over time and **Blue dashed-lined** plots - the value of U_2 control measures over time respective to provinces.

The red-lined plots in Figure 8 show the number of infected individuals over time when considering the control measure. By implementing the maximum control measure it takes a maximum of nearly 40 days

to control the disease burden. The corresponding value of the control measure is represented in the blue dashed-lined plots in Figure 8. To control the disease burden it takes 40 - 50 days.

Compared to the previous sub-section 3.3.1, vaccination takes less time to control the disease. Since vaccination does not disturb the lives of the general community rather than social distancing, vaccination will be the most efficient control strategy.

3.4. Results in the presence of control measures

The results are analyzed in this section using the model described in Equations 2 and 3. Sensitivity analysis is designed to capture the behavior of the disease when presenting control measures. The different relative weights for the control measures are considered in the simulation in order to identify the optimal solution that reduces the disease burden while minimizing the costs associated with control measures and infected individuals. As a result of the previous Sub-section 3.3, vaccination controls the disease burden compared to social distancing. Following Figures 9, 10, 11, 12, and 13 show the behavior of the disease spread when using the different relative cost weights for the $u_{1i} \quad and \quad u_{2i}$. The $W_1 \quad and \quad W_2$ are positive relative constants according to the $u_{1i} \quad and \quad u_{2i}$ respectively.

1) ***Simulation 1: Relatively high weight for vaccination****:* Weight of the control measures as follows: Set $W_1 = 0.1 \quad and \quad W_2 = 0.9$. In the first days of the time interval, control measures are implemented at their maximum capacities. As shown in Figure 9 red-lined plots represent the infected individual over time and blue-dotted-line and orange dashed-lined plots represent the corresponding values of control measures over time with respective provinces. Under the maximum control, 30 to 40 days are taken to control the disease burden.

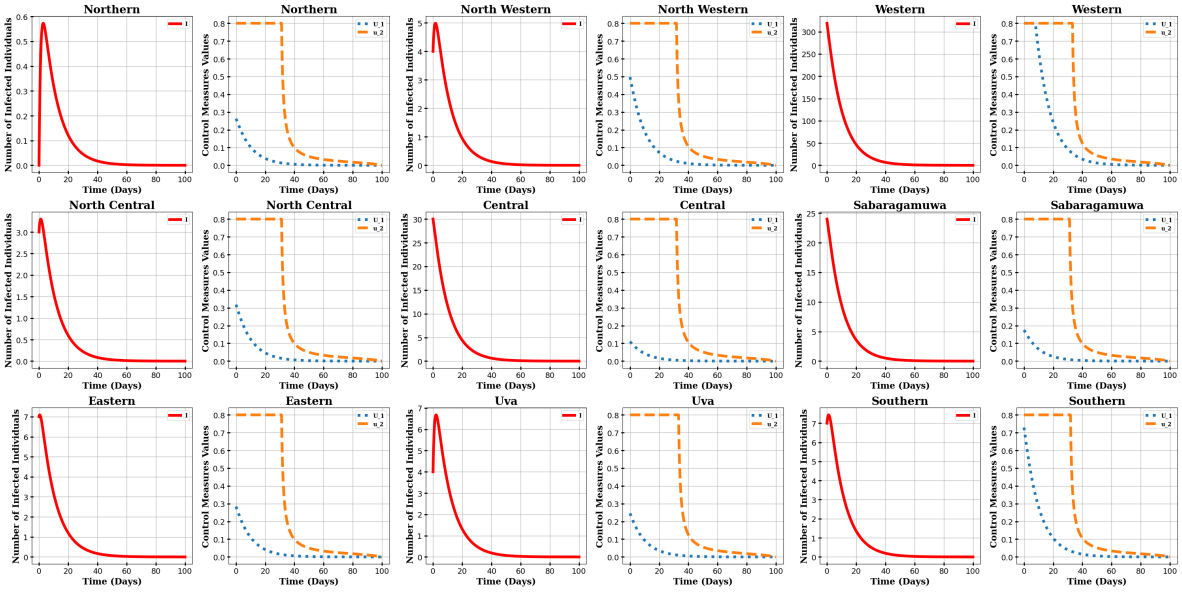

Figure 9: **Red lined** plot - Infected individuals over time and **Blue dotted-line and Orange dashed-lined** plots - Control measures over time for simulation 1 with respective provinces.

Initially, both control variables are used at their maximum capacities according to the risky provinces such as the Western province. After obtaining the control, it reduces the control values within 85 - 100 days. The u_{1i} is used with maximum capacity in the first 10 days in Western. Southern and Northern West have to use 70% and 50% in the first days of the period respectively. Other provinces have to use less than 50% level of u_{1i} to control the disease burden. The u_{2i} has to be implemented at its maximum capacity first 10 days for all provinces. According to the plots Western and Southern provinces can be considered as the most critical

provinces. The weight of vaccination is higher but to reduce the disease burden vaccination could be selected as the most suitable control measure.

2) ***Simulation 2: Weight of social distancing as 0.3 and 0.7 as cost of vaccination****:* Weights for cost allocation are $W_1 = 0.3 \quad and \quad W_2 = 0.7$. Red, Blue- dotted, and Orange-dashed-lined plots in Figure 10 show the infected individuals, corresponding u_{1i} and u_{2i} overtime respectively. In this case, maximum capacities of control measures are used in between 30 - 40 days. Between the weight for the u_{1i} and the implementing amount of u_{1i} has an inversely proportional relationship. Only Western has to use u_{1i} at the level of 60% in the first days of the period and other provinces implement u_{1i} less than 30%.

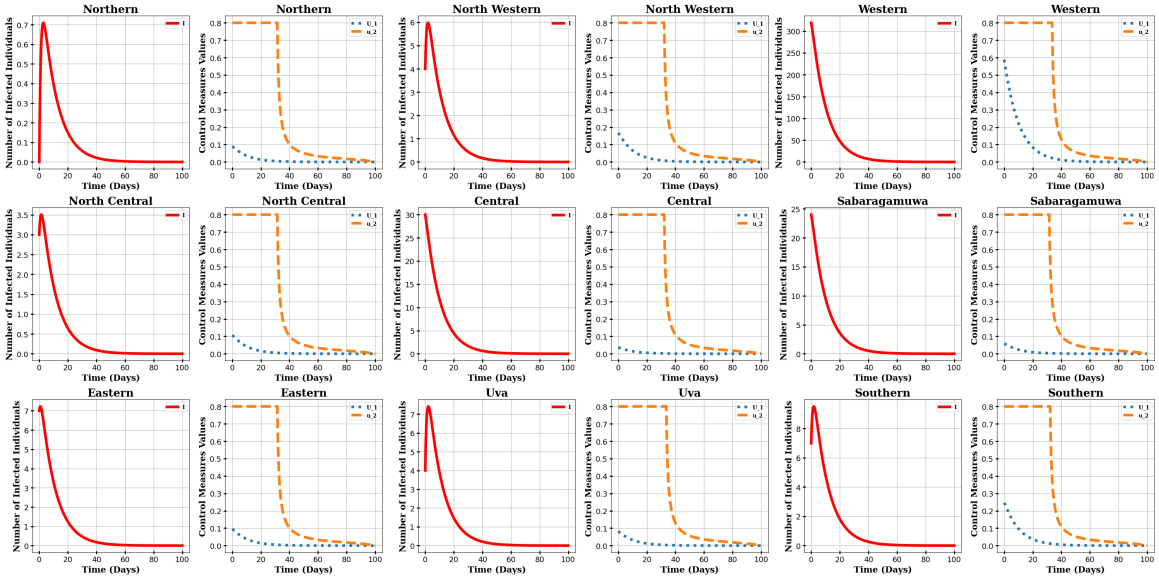

Figure 10: **Red lined** plot - Infected individual over time and **Blue dotted-line and Orange dashed-lined** plots - Control measures over time for simulation 2 with respective to provinces.

3) ***Simulation 3: Equal weights for both control measures****:* Weights are defined as equal costs for both control measures $W_1 = W_2 = 0.5$.

Red-lined plots in Figure 11 represent the infected individuals over time. The number of infected individuals is less than in the previous simulations. Blue-dotted-lined plots in Figure 11 show the control measure u_{1i} varies with time and it has been used relatively less than the previous simulations. But in Orange-dashed-lined plots in Figure 11 represent the control measure u_{2i} and it is used relatively more than the previous simulations. The reason for the variation of weights for u_{1i} is increasing and weights for the u_{2i} are decreasing compared to the previous simulations.

Vaccination is used at its maximum capacity of less than 35 - 40 days. Most provinces are able to end the partial lockdown within 20 days and in risky provinces, it takes 40 days. It takes about 90-100 days to control the disease burden and that is a higher count of days comparatively with the previous simulation. The behavior of the control measures in provinces other than Western and Southern provinces is almost the same.

4) ***Simulation 4: Weight of social distancing as 0.7 and 0.3 as cost of vaccination****:* When increasing the weight of u_{1i}, the values of the measure decrease. The total number of days to implement the control measure remains the same.

Vaccination is used for nearly 40 days with its maximum capacity to control the disease burden. Because the cost of social distancing is high, less than 50% of this control measure is used in the Western province, which was identified as a risky province in the previous simulations. Other provinces implement u_{1i} less than 20%.to 5%. The behavior of control measures, detailed representation can be seen in blue dotted-line

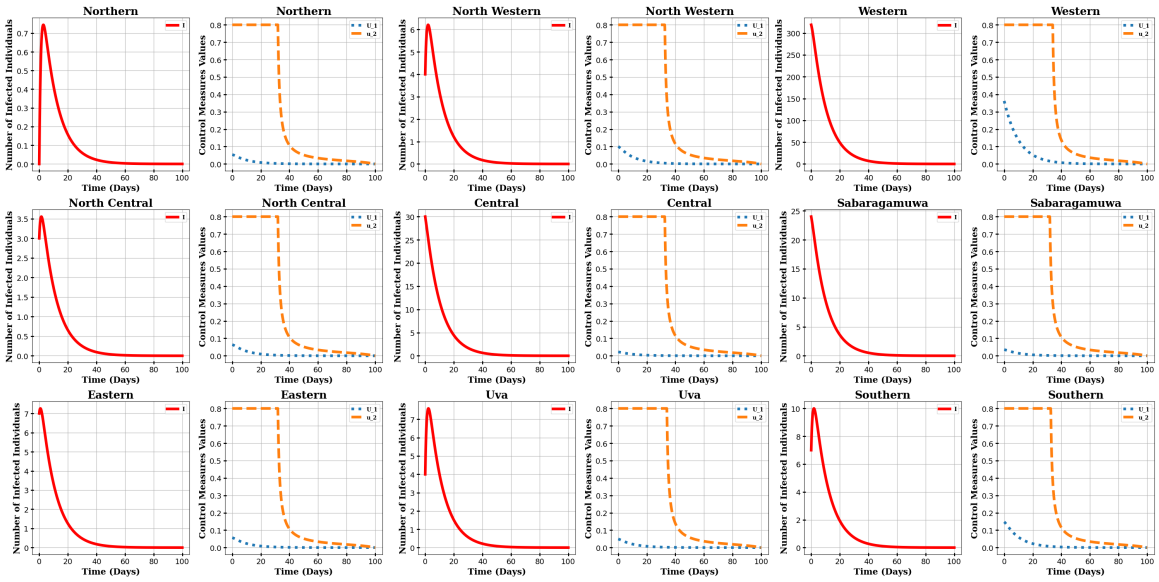

Figure 11: **Red lined** plot - Infected individual over time and **Blue and Orange** plot - Control measures over time for simulation 3 with respective to provinces.

and orange dashed-lined in Figure 12. In this simulation, vaccination is a more active control measure than the other.

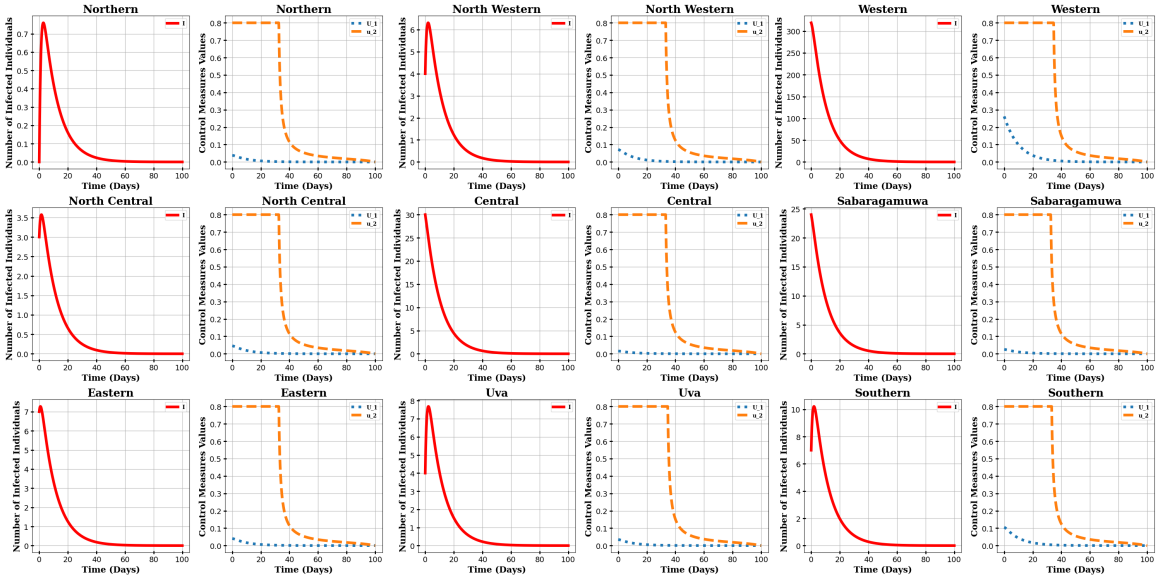

Figure 12: **Red lined** plot - Infected individuals over time and **Blue dotted-line and Orange dashed-lined** plots - Control measures over time for simulation 4 with respective to provinces.

5) ***Simulation 5: Relatively high weight for social distancing****:* The weight for u_{1i} *and* u_{2i} are equal to 0.9 and 0.1 respectively. As the result of Sub-section 3.3, we have to give more priority to vaccination than to social distancing. Infected individuals over time are shown in Figure 13 in red-lined plots and control

measures over time are shown in Figure 13 in blue-dotted and orange-dashed-lined. Nearly 40 days will be taken to control disease within all patches with maximum capacity of vaccination. Even Western province has less than 20% implementing level shown in Figure 13. The control measure in the social distance is a lower value in this situation in risky patches. In low-risk patches, the value of the control measure approaches zero due to the weight of u_{1i} being more than the others. The behavior of both control measures all almost the same as are the provinces.

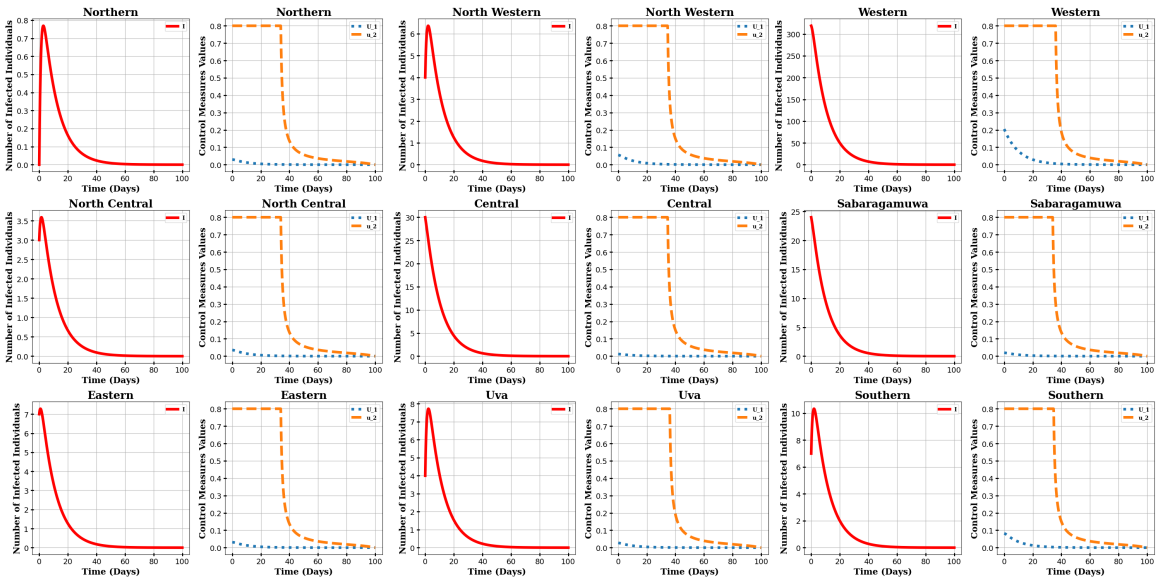

Figure 13: **Red lined** plot - Infected individuals over time and **Blue dotted-line and Orange dashed-lined** plots - Control measures over time for simulation 5 with respective to provinces.

Figure 14 shows the variation of R_t over time for simulations 1, 2, 3, 4, and 5 in subsection 3.4 respectively. The effective reproduction number R_t is interested in understanding the relationship between the control measures and the size of the disease burden. The equation of R_t in the subsection 2.2, describes the relationship between R_t and u_{1i} are inversely proportional. When increasing the W_1, the value at the initial point of R_t also increases. As a result of this, we can identify vaccination is more effective than social distancing in minimizing the disease burden and the cost of control measures.

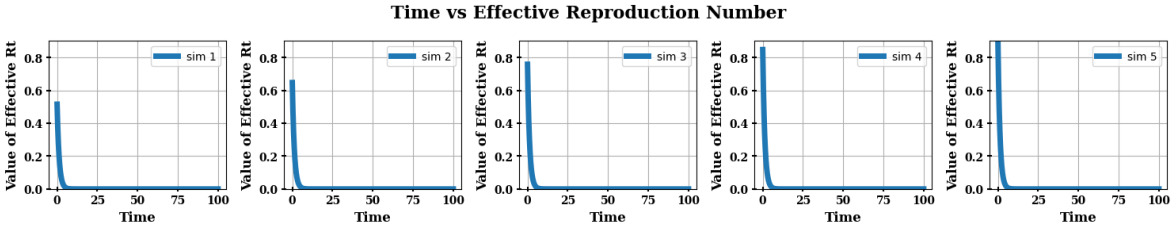

Figure 14: Effective reproduction number over time for all simulations.

Figure 15 shows the final epidemic size for each simulation in presence control measures. According to the following Figure15, the final epidemic size of simulation 3.4.1 for each patch is higher than the other simulations. The relationship between the final epidemic size and the total cost is directly proportional and it is described in subsection 2.2. Furthermore, the final epidemic size represents the patch-specific cost value for infected individuals. Specifically, it supports decision-makers in maintaining and continuing the government

and private health care system. R_t represents the overall idea of the population and the prediction of secondary cases and the final epidemic size represents the patched-specified cost value for infected individuals. Therefore, when studying meta-population or multi-patches, it is important to analyze the results of the final epidemic size.

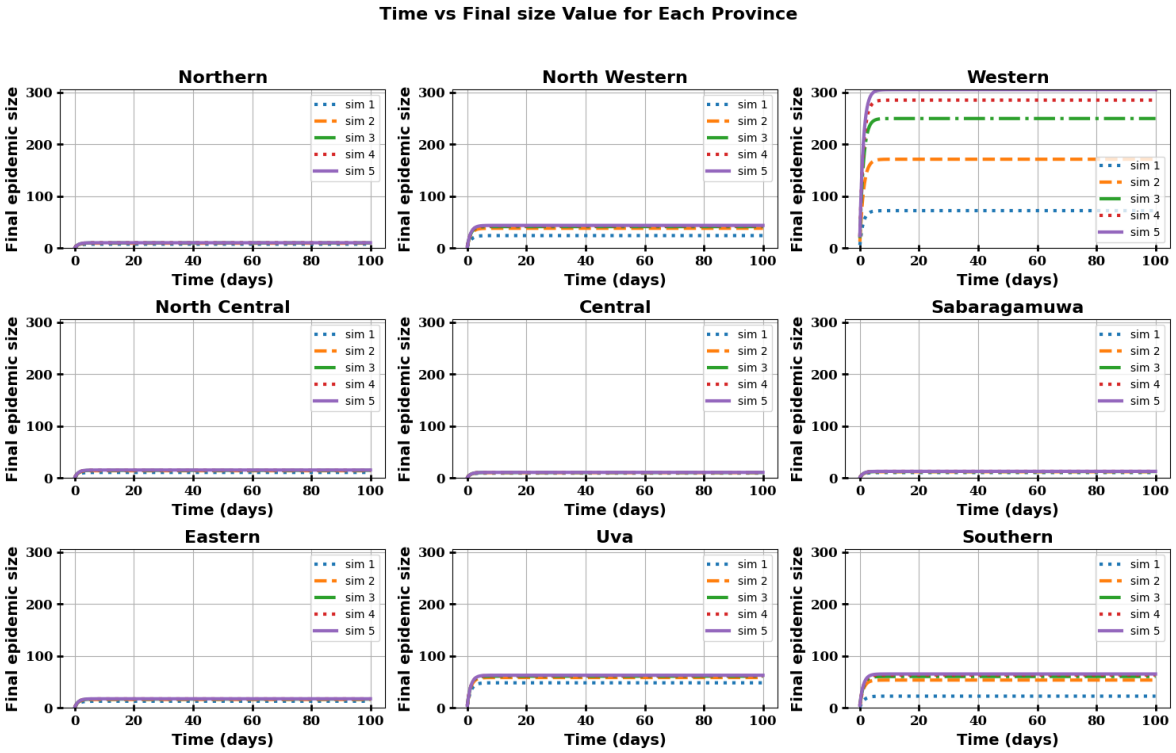

Figure 15: Final epidemic size when the presence of control measures.

4. Discussion

Modeling the spread of the disease in meta-population is setting the model to real-world situations. Multiple patches are interconnected by human mobility. Mobility behaviors play a significant role in disease spread [3]. The optimal control theory is employed to identify the appropriate control strategies to reduce the size of the outbreak while minimizing the costs of implementing the control measures [4].

First, we analyze the spreading of the disease in the long run without any control measures in sub-section 3.2. According to this situation, the R_t indicates 1.1 and it is a pandemic situation. After nearly 750 to 1000 days without any control strategies, the rate of spreading disease reaches 1.0. At that point, the disease has been controlled but does not die out. In Sub-section 3.3, we analyze by considering u_{1i} and u_{2i} separately. Table 4 shows the summary of the results of this section.

Table 4: Summary of results when considering control measures separately.

Control measure	Days to control the disease burden	Days to use maximum capacity
Only using u_{1i}	more than 150	50 days full national lockdown 50-80 partially lockdown
Only using u_{2i}	40-50	Nearly 40

When considering only u_{1i}, 30 days of national-wise lockdown and 30-80 days of full and partial lockdown are not appropriate in a low-income country such as Sri Lanka. According to the result shown in Table 4, relative to u_{1i}, the disease can be controlled by u_{2i}.

Then the summary of Section 3.4 is shown in Table 5. Scenarios are defined based on different weights for the cost of control measures u_{1i} and u_{2i}.

Table 5: Summary of results when the presence of controls measures.

W_1	W_2	R_t	Days to control the disease	Max. days of u_{1i}	Max. days of u_{2i}
0.1	0.9	0.5	85 - 100	10	30 - 40
0.3	0.7	0.6 - 0.7	80-100	-	30 - 40
0.5	0.5	0.75 - 0.8	90-100	-	35 - 40
0.7	0.3	0.85	Nearly 100	-	40
0.9	0.1	0.8 - 0.9	100 or nearly above days	-	Nearly 40

The relationship between the value of W_1 and the implementing level of u_{1i} is inversely proportional. u_{1i} contributes its maximum capacity in the first simulation, but in the last simulation, it contributes less than 20%. As a result of the Section 3, we identified u_{2i} is controlled by the disease relatively more than the u_{1i}. As shown in Table 5 more weight is placed on u_{1i}, and the time taken to eliminate the disease increases. And that is also confirmed by the variation of the R_t.

The important points found in the research are summarized as follows: the multi-patch epidemic model with the human dispersal behavior approach model to be more realistic. By incorporating the optimal control theory it captured patch-specified optimal values for implementing control measures. And it helped policy-makers to decide the optimal solution while minimizing the disease burden and minimizing cost. According to the analysis result, the disease can be controlled by vaccination compared to social distancing. Compared to the basic reproduction number (R_0), the effective reproduction number (R_t) represents the significant result in the epidemiological model incorporated with control measures. R_t indicates the overall idea of the population and the final epidemic size represents patched-specified values. Therefore, when studying meta-population or multi-patches, it is important to analyze the results of the final epidemic size.

From these models, we provide sensitive optimal solutions regarding the COVID-19 pandemic situation in Sri Lanka. In addition to supporting the decision-making process related to continual health service in both the public and private sectors as well as maintaining the nation's economy.

5. Future work

In this research, we formulate a multi-patch SIR model to control and reduce communicable disease outbreaks such as COVID-19 by optimizing resource allocation in Sri Lanka. The next step is to formulate a compartmental model such as SEIR, SAEIR, and SITR, which will be able to capture more complex situations as well as more real situations.

References

[1] Lee, S., Baek, O. and Melara, L., Resource allocation in introduction-patch epidemic model with state-dependent dispersal behaviors using optimal control, Processes, 8(9), p. 1087, 2020.

[2] Brauer, F., Castillo-Chavez, C., Feng, Z., Brauer, F., Castillo-Chavez, C. and Feng, Z., Epidemiological models incorporating mobility, behavior, and time scales, Mathematical Models in Epidemiology, pp. 477-504, 2019.

[3] Funk, S., Salath´e, M. and Jansen, V.A., Modelling the influence of human behaviour on the spread of infectious diseases: a review, Journal of the Royal Society Interface, 7(50), pp. 1247–1256, 2010.

[4] Martcheva, M., An introduction to mathematical epidemiology, Springer, 61, pp. 9-31, 2015.

[5] Asano, E., Gross, L.J., Lenhart, S. and Real, L.A., Optimal control of vaccine distribution in a rabies metapopulation model, Mathematical Biosciences and Engineering, 5(2), pp. 219-238, 2008.

[6] Okyere, E., Olaniyi, E. and Bonyah, E., Analysis of zika virus dynamics with sexual transmission route using multiple optimal controls, Scientific African, 9, p. e00532, 2020.

[7] Erandi, K., Mahasinghe, A.C., Perera S. and Jayasinghe, S., Effectiveness of the strategies implemented in Sri Lanka for controlling the Covid-19 outbreak, Journal of Applied Mathematics, 2020(1), pp. 1–10, 2020.

[8] Ahmad, M.D., Usman, M., Khan, A. and Imran, M., Optimal control analysis of ebola disease with control strategies of quarantine and vaccination, Infectious Diseases of Poverty, 5, pp. 1–12, 2016.

[9] Makinde O.D. and Okosun, K.O., Impact of chemo-therapy on optimal control of malaria disease with infected immigrants, BioSystems, 104(1), pp. 32-41, 2011.

[10] Singh, A. and Chattopadhyay, A., COVID-19 recovery rate and its association with development, Indian Journal of Medical Sciences, 73(1), p. 8, 2021.

[11] Swarnamali, H., Francis, T.V., Sooriyaarachchi, P. and Jayawardena, R., COVID-19 vaccine hesitancy in Sri Lanka: A national level survey, International Journal of Health Sciences, 17(1), p. 3, 2023.

[12] Lenhart, S. and Workman, J.T., Optimal control applied to biological models, CRC Press, 2007.

[13] ElHassan, A., AbuHour, Y. and Ahmad, A., An optimal control model for covid-19 spread with impacts of vaccination and facemask,Heliyon, 9(9), 2023.

[14] Mahasinghe, A., Erandi, K. and Perera, S., An optimal lockdown relaxation strategy for minimizing the economic effects of covid-19 outbreak, International Journal of Mathematics and Mathematical Sciences, 2021(1), pp. 1-10, 2021.

[15] Güner, H.R., Hasanoğlu, İ. and Aktaş, F., COVID-19: Prevention and control measures in community, Turkish Journal of Medical Sciences, 50(9), pp. 571-577, 2020.

[16] WHO, Advice for the public on Covid-19. https://www.who.int/emergencies/diseases/novel-coronavirus-2019/advice-for-public, Accessed on December 7, 2024.

[17] WHO, Covid-19 weekly epidemiological update. https://www.epid.gov.lk/storage/post/pdfs/en_64f33bb8771c9_sitrep-gl-en-02-09_10_23.pdf,2023, Accessed on December 6, 2023.

[18] Amaratunga, D., Fernando, N., Haigh, R. and Jayasinghe, N., The Covid-19 outbreak in Sri Lanka: A synoptic analysis focusing on trends, impacts, risks and science policy interaction processes, Progress in Disaster Science, 8, p. 100133, 2020.

[19] Mahasinghe, A.C., Erandi, K. and Perera, S., An optimal lockdown relaxation strategy for minimizing the economic effects of covid-19 outbreak in sri lanka, This Version Posted June, 9, p. 2020, 2020.

[20] Watson, O.J., Barnsley, G., Toor, J., Hogan, A.B., Winskill, P., and Ghani, A.C., Global impact of the first year of Covid-19 vaccination: a mathematical modelling study, The Lancet Infectious Diseases, 22(9), pp. 1293–1302, 2022.

[21] Epidemiology Unit, Vaccination summary. https://www.epid.gov.lk/vaccination-summary, Accessed on September 1, 2023.

[22] King, W.G., The prevention of malaria, British Medical Journal, 1(2631), p. 1348, 1911.

[23] Hsieh, Y.H., Van den Driessche, P. and Wang, L., Impact of travel between patches for spatial spread of disease, Bulletin of Mathematical Biology, 69, pp. 1355-1375, 2007.

[24] Rushton, S. and Mautner, A.J., The deterministic model of a simple epidemic for more than one community, Biometrika, 42(1/2), pp. 126-132, 1955.

[25] Bichara, D., Kang, Y., Castillo-Chavez, C., Horan, R. and Perrings, C., SIS and SIR epidemic models under virtual dispersal, Bulletin of Mathematical Biology, 77, pp. 2004-2034, 2015

[26] Nuha, A.R., Achmad, N., Rahman, G.A., Abdullah, S., Chasanah, S.I.U. and Valentika, N., Analysis of optimum control on the implementation of vaccination and quarantine on the spread of covid-19, BAREKENG: Jurnal Ilmu Matematika dan Terapan, 16(4), pp. 1139-1146, 2022.

[27] Firmansyah, F. and Rangkuti, Y.M., Sensitivity Analysis and Optimal Control of Covid 19 Model, Jambura Journal of Biomathematics (JJBM), 4(1), pp. 95-102, 2023.

[28] Sattenspiel, L. and Dietz, K., A structured epidemic model incorporating geographic mobility among regions, Mathematical Biosciences, 128(1-2), pp. 71-91, 1995.

[29] Lee, S. and Castillo-Chavez, C., The role of residence times in two-patch dengue transmission dynamics and optimal strategies, Journal of Theoretical Biology, 374, pp. 152-164, 2015.

[30] Bock, W. and Jayathunga, Y., Optimal control of a multi-patch dengue model under the influence of Wolbachia bacterium, Mathematical Biosciences, 315, p. 108219, 2019.

[31] Erandi, K.K.W.H., Mahasinghe, A.C., Ganegoda, N.C., Perera, S.S.N. and Jayasinghe, S., Identifying long–term optimal vaccination strategies for mitigating a pandemic: a computational modeling approach using covid-19 data in srilanka, Communications in Combinatorics, Cryptography and Computer Science, 2023(1), pp. 20-28, 2022.

[32] Department of Census and Statistics - Sri Lanka, Census map - Sri Lanka, 2023. http://map.statistics.gov.lk:8080/LankaStatMap/apps/gs/censusmap/index.html, Accessed on December 6, 2023.

[33] Heffernan, J.M., Smith, R.J. and Wahl, L.M., Perspectives on the basic reproductive ratio, Journal of the Royal Society Interface, 2(4), pp. 281-293, 2005.

[34] Wallinga, J. and Teunis, P., Different epidemic curves for severe acute respiratory syndrome reveal similar impacts of control measures, American Journal of Epidemiology, 160(6), pp. 509-516, 2004.

[35] Caicedo-Ochoa, Y., Rebellón-Sánchez, D.E., Peñaloza-Rallón, M., Cortés-Motta, H.F. and Méndez-Fandiño, Y.R., Effective Reproductive Number estimation for initial stage of COVID-19 pandemic in Latin American Countries, International Journal of Infectious Diseases, 95, pp. 316-318, 2020.

[36] Barratt, H., Kirwan, M., and Shantikumar, S., Epidemic theory (effective and basic reproduction numbers, epidemic thresholds) and techniques for analysis of infectious disease data (construction and use of epidemic curves, generation numbers, exceptional reporting and identification of significant clusters), Health Knowledge, 2018.

[37] Epidemiology Unit, Covid-19 disease surveillance and vaccination. https://www.epid.gov.lk/covid-19-data, Accessed on December 6, 2023.

[38] Ministry of Finance Sri Lanka, https://www.treasury.gov.lk/budget#estimates, Accessed on December 6, 2023.

[39] SciPy Developers, scipy.optimize.least squares-scipy v1.8.0 reference guide, https://docs.scipy.org/doc/scipy/reference/generated/scipy.optimize.least_squares.html, Accessed on March 14, 2024.

[40] National Transport Commission, https://www.transport.gov.lk/web/index.php?option=com_content&view=article&id=27&Itemid=147&lang=en#private-bus-operational-data-inter-intra-provincial, Accessed on December 6, 2023.

[41] Sri Lanka Transport Board, https://www.transport.gov.lk/web/index.php?option=com_content&view=article&id=25&Itemid=145&lang=en#no-of-passengers-transportedl, Accessed on December 6, 2023.